



TECHNICAL ARTICLE

# Structure and Corrosion Resistance Characteristics of ZnAl/EP Coating on Bonded NdFeB Magnet

Youwen Yang, Nan Jiang, Yingzhong Sun, Lei Yang, Chuanhai Guan, Enhua Zhang, Xiaogang Fang, and Jiguang Liu

Submitted: 18 March 2022 / Revised: 15 August 2022 / Accepted: 9 September 2022 / Published online: 3 October 2022

ZnAl/epoxy resin (ZnAl/EP) composite coating with a thickness of 30.5  $\mu\text{m}$  was prepared on bonded NdFeB magnetic ring. The morphologies and composition of ZnAl-EP/NdFeB were characterized by scanning electron microscopy (SEM) and energy-dispersive spectroscopy (EDS). The surface roughness of samples was measured by 3D Laser Confocal Scanning Microscope (LCSM). The samples of prepared EP/NdFeB and ZnAl-EP/NdFeB were used for corrosion tests in potentiodynamic polarization method, electrochemical impedance spectroscopy (EIS) and neutral salt spray (NSS) test. The magnetic properties of samples were measured with a permanent magnet material measuring instrument. The corrosion current density ( $J_{corr}$ ) of ZnAl-EP/NdFeB is 1 order of magnitude lower than that of EP/NdFeB, reflecting the corrosion resistance of ZnAl-EP/NdFeB is much higher in contrast with the EP/NdFeB. Compared with the EP/NdFeB, the NSS test time of ZnAl-EP/NdFeB is increased from 72 to 936 h. In addition, the ZnAl-EP coating has no significant effect on the magnetic properties of NdFeB magnetic ring.

**Keywords** air spraying, bonded NdFeB, cathodic electrophoretic deposition, corrosion resistance, ZnAl-EP coating

## 1. Introduction

As the third generation of rare earth permanent magnet materials, NdFeB magnets have excellent magnetic properties and they have been in great demand in many fields such as in communication, automation, instrument control, new energy automobile, computer hard disk drives and wind power turbines (Ref 1-3). However, the large electrochemical potential difference among the matrix phases and the active chemical properties of the neodymium-rich phase in NdFeB magnets make its corrosion resistance greatly damaged (Ref 4, 5). At present, the methods dedicated to improving the corrosion resistance of NdFeB magnets mainly include alloy methods and surface coating methods (Ref 6). The alloy method is to dope Al, Co, Ce and other elements into the magnet to reduce the potential difference between principal and non-principal phases and improve the corrosion resistance of the magnet (Ref 7, 8). Nonetheless, although doping alloy elements can improve the

anti-corrosion performance of NdFeB magnet, the improvement in anti-corrosion performance is often accompanied by a deterioration of magnetic properties (Ref 9). The coating cladding preparation techniques mainly include electroplating, physical vapor deposition and cathode electrophoresis (Ref 10-12). Previous studies indicated that the electroplating process can enhance the corrosion resistance of sintered NdFeB magnets while it can bring some problems such as environmental pollution, poor adhesion, blistering and hydrogen embrittlement (Ref 13, 14). Physical vapor deposition can modify the coating, yet high equipment costs and low production efficiency restrict its development (Ref 15). Under the premise of fully considering environmental protection, cost and coating performance, electrophoretic deposition is currently the most widely used coating preparation technology in the NdFeB surface protection field.

The NdFeB corrosion-resistant coating mainly includes three groups: metallic coating, polymer coating and composite coating. The metallic coating is to coat Zn, Al, Ni and other metals on the surface of NdFeB magnets by various methods (Ref 16, 17). Li et al. (Ref 18) deposited a Al layer on the surface of the sintered NdFeB by magnetron sputtering, and the result revealed that the Al layer has excellent protective properties. Nonetheless, the Al layer had low hardness and was easily mechanically scratched. Zhang et al. (Ref 19) found that although the single silane film had a good surface protection effect, its mechanical properties were not ideal. The coating had local cracks and other defects, and its wear resistance was poor. To overcome the shortcomings of metallic or polymer single coating, metallic/polymer composite coatings have been conducted to further improve the anti-corrosion performance of the NdFeB magnets. Liu et al. (Ref 20) prepared Zn/silane composite coatings on the surface of sintered NdFeB magnet utilizing electrodeposition. The result showed that the  $J_{corr}$  of the composite coatings was 1 order of magnitude lower than that of the single Zn coating, and the NSS test time reached 192 h. Chen et al. (Ref 21) prepared a zinc oxide whisker/

**Youwen Yang, Xiaogang Fang, and Jiguang Liu**, School of Materials Science and Engineering, Hefei University of Technology, Hefei 230009 Anhui Province, People's Republic of China; and Engineering Research Center of High-Performance Copper Alloy Material and Forming, Ministry of Education, Hefei University of Technology, Hefei 230009 Anhui Province, People's Republic of China; **Nan Jiang, Yingzhong Sun, and Lei Yang**, School of Materials Science and Engineering, Hefei University of Technology, Hefei 230009 Anhui Province, People's Republic of China; **Chuanhai Guan and Enhua Zhang**, Anhui Constant Magnetic Magnetolectricity Co., Ltd., Luan 239000 Anhui Province, People's Republic of China. Contact e-mail: hfutyw@hfut.edu.cn.

polydimethylsiloxane-micro-arc oxidation (T-ZnOw/PDMS-MAO) composite coating via MAO treatment combined with spraying T-ZnOw/PDMS on sintered NdFeB magnet. The result displayed that the  $J_{corr}$  of the composite coating was 3 orders of magnitude lower than the MAO coated NdFeB. Obviously, metallic/polymer composite coating is one of the effective ways to improve the corrosion resistance of NdFeB magnets.

With the expansion of application fields, such as new energy vehicle motors, it is critical to improve the corrosion resistance of the bonded NdFeB magnets. To the best of our knowledge, the relevant metal and polymer composite coatings were concentrated on sintered NdFeB, but not involved in bonded NdFeB. As a kind of dacrocoat coating, ZnAl coating is often used to prepare the surface protective coatings of metal and NdFeB magnets to improve their mechanical properties and corrosion resistance (Ref 22, 23). In our previous research (Ref 24), we have prepared the ZnAl coating on the surface of the NdFeB magnetic rings. And the NSS time of the coating reached 264 h, which demonstrated good corrosion resistance. In order to make the coating obtain more excellent structure and performance, in this paper, the surface of the bonded NdFeB magnet ring was coated with ZnAl/epoxy resin (ZnAl/EP) composite coating by air spraying combined with electrophoretic deposition process for the first time. The structural characteristics and corrosion resistance of the EP/NdFeB and ZnAl-EP/NdFeB were studied and analyzed in detail as well as the magnetic properties.

## 2. Experimental

### 2.1 Preparation of NdFeB Magnetic Rings

The bonded NdFeB magnetic rings with the size of  $20.2 \times 18.7 \times 7$  mm (OD  $\times$  ID  $\times$  H) were manufactured by compression molding method. The raw material used for the magnetic rings was the NdFeB mixed magnetic powders, which was uniformly mixed with MQP-12-8HD (11.5 wt.% Nd, 72.0 wt.% Fe, 1.1 wt.% B, 9.9 wt.% Ce, 3.8 wt.% Pr and 1.7 wt.% Zr) magnetic powders and MQP-14-12 (26.0 wt.% Nd, 71.1 wt.% Fe, 1.0 wt.% B and 1.9 wt.% Nb) magnetic powders (supplied by Magnequench (Tianjin) Co., Ltd.) in a ratio of 1:1. After being pressed, the magnetic rings were cured for 13 min in a high-temperature tunnel furnace at 190 °C. After being chamfered and polished, the NdFeB rings were cleaned and dried by an ultrasonic cleaner for 20 min at 120 °C and then cooled naturally to room temperature.

### 2.2 Preparation of ZnAl-EP Coating

In the past research, we have used the air spraying process to prepare the ZnAl coating on the surface of the bonded NdFeB magnetic rings (Ref 24). The spraying amount of the coating solution was 28/30 s, and the spraying pressure was 0.3 MPa. The magnetic rings need to be sprayed twice for 1.5 min each. The magnetic rings sprayed on both sides were solidified in the infrared curing oven at 230 °C for 45 min. In order to prepare the ZnAl-EP composite coating, the EP coating was cladded on the surface of the ZnAl/NdFeB by electrophoretic deposition. The coating used in the electrophoresis process was epoxy paint (SEPD-7-001), which was mixed with cation electrocoat resin (CR691B/200 K-Cl, 47.6 wt.%), solvent (PPGSOLVENT-03/

16 K-Cl, 1.0 wt.%), cation electrocoat paste (CP522F/280 K-Cl, 7.0 wt.%) and pure water (44.4 wt.%). Firstly, the ZnAl/NdFeB was washed with pure water and then immersed in the electrophoresis bath (the electrophoresis voltage and the temperature were 110 V and 28 °C for 2 min). Secondly, the magnetic ring was sprayed with foam and washed with pure water, and then, the surface water was blown off with an air gun. Finally, the magnetic ring was placed in the furnace of the vault and baked for 20 min at 170 °C. For comparison, we also specially prepared the EP/NdFeB using the same process.

### 2.3 Characterization and Test

The surface and cross-sectional morphologies of EP/NdFeB and ZnAl-EP/NdFeB coatings were characterized by field emission SEM (SU8020, Hitachi), and the components of ZnAl-EP composite coating were analyzed by EDS. The 3D Laser Confocal Scanning Microscope (LCSM, VK-X250, Japan) was used to analyze the surface roughness of the coating. The electrochemical workstation (Shanghai Chenhua, CHI760E, China) was used for the potentiodynamic polarization and EIS tests. Before the polarization test, divide the annular samples into several magnetic slices with radians. On the premise of not damaging the surface to be tested and ensuring the accuracy of the test results, the inner circular surfaces of the magnetic slices were ground and thinned into a rectangle with dimension accuracy of  $7 \times 6$  mm by metallographic sandpaper. Then, the surrounding five sides of the samples were sealed with metallographic mosaic material to ensure that the test working area was  $0.42 \text{ cm}^2$  and would not affect the test results. The samples were immersed in 3.5 wt.% NaCl solution for 1 h to make them reach a stable chemical potential, and then, the test was carried out. A three-electrode system was used for the electrochemical test, and the scanning potential was  $-1.4$ – $0.5$  V (the scanning rate was  $0.005$  V/s). The NSS test was studied by the salt spray corrosion test chamber (AHL-90-CSF) with 5 wt.% NaCl solution at  $35 \pm 2$  °C. When the specimen has the first visible corrosion product, the corresponding time is the NSS resistance time. At last, a permanent magnet material measuring instrument (NIM-200C) was used to measure the remanence ( $B_r$ ), intrinsic coercivity ( $H_{ci}$ ) and magnetic energy product ( $(BH)_{max}$ ) of bare NdFeB, EP/NdFeB and ZnAl-EP/NdFeB.

## 3. Results and Discussion

### 3.1 Morphology Characterization

Figure 1 shows the surface morphologies and surface profiles of bare NdFeB, EP/NdFeB and ZnAl-EP/NdFeB, respectively. It is observed that the surface of the bare NdFeB is coarse and has an irregular block-like crystal structure (Fig. 1a). There are plentiful of pores among the crystal grains and the gaps vary from 1 to 10  $\mu\text{m}$ . The rough surface of bare NdFeB can also be further reflected from the surface profile, as shown in Fig. 1(b). It can be seen that the predominantly gray surface is scattered with red and blue areas, indicating that the surface of bare NdFeB has large undulation. Through software determination, the average surface roughness ( $S_a$ ) of bare NdFeB is  $1.146 \mu\text{m}$ . As shown in Fig. 1(c), under the protection of EP particles, the surface of EP/NdFeB becomes smooth, and there are hardly any noticeable cracks and holes on

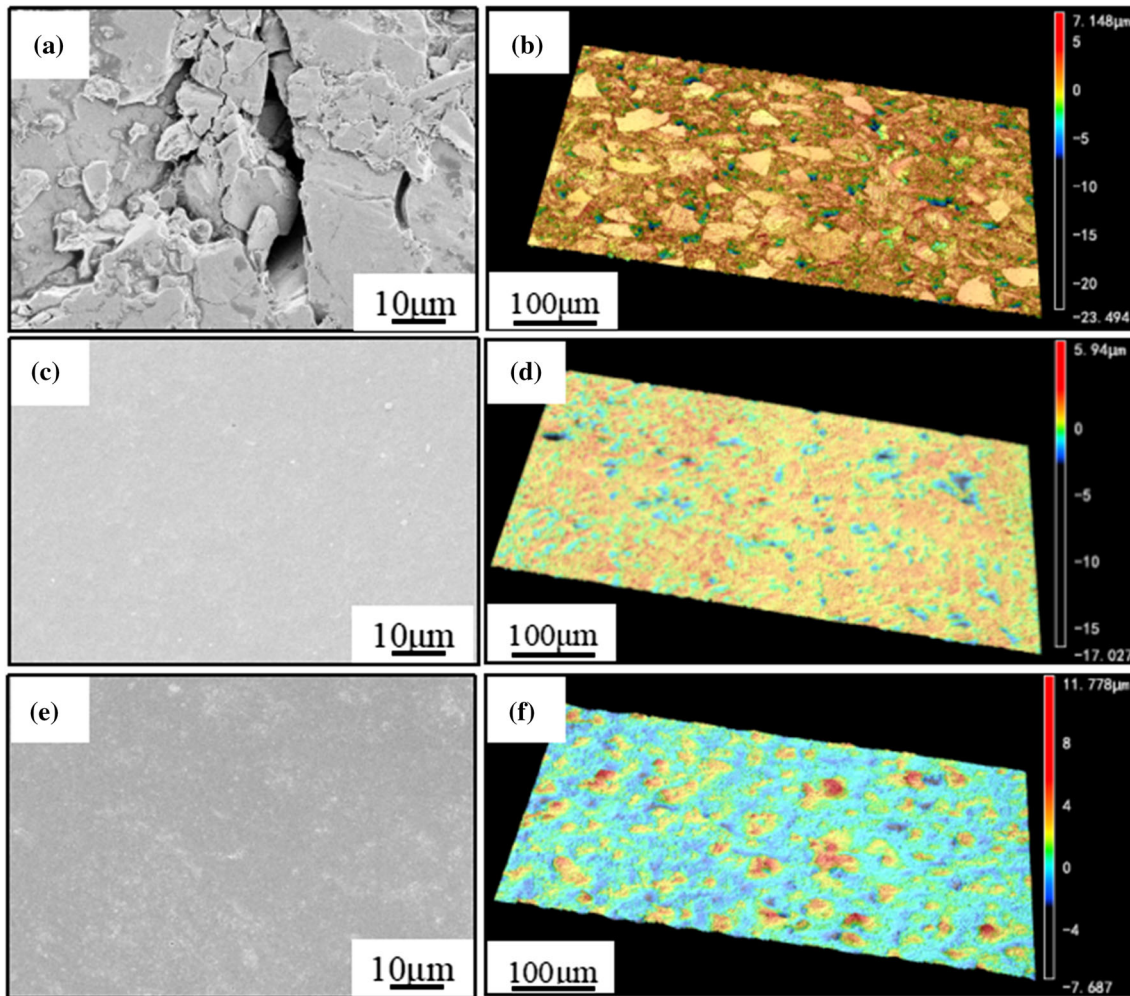


**Fig. 1** SEM surface morphologies and surface profiles of NdFeB (a,b), EP/NdFeB (c,d) and ZnAl-EP/NdFeB (e,f)

the surface of the coating. The  $S_a$  of EP/NdFeB is  $0.635 \mu\text{m}$ , which is only half of that of bare NdFeB (Fig. 1d). We can see that the red peaks in the figure are dense, indicating that there are many bumps on the surface of EP/NdFeB. Compared with the bare NdFeB, the  $S_a$  of EP/NdFeB is lower, which effectively delays the corrosion tendency of the magnetic ring surface. Compared with the EP/NdFeB, the  $S_a$  of ZnAl-EP/NdFeB is slightly increased to  $1.098 \mu\text{m}$  (Fig. 1f). In our previous research (Ref 24), the  $S_a$  of ZnAl/NdFeB exceeded  $2 \mu\text{m}$ , which was much greater than the  $S_a$  of EP/NdFeB. In this study, the EP coating was cladded on the surface of the ZnAl/NdFeB by electrophoretic deposition. It can be seen that the EP layer greatly reduced the  $S_a$  of the ZnAl surface. After the EP layer was deposited on the surface of ZnAl coating, EP particles effectively filled the pores of ZnAl coating, and the surface of ZnAl-EP/NdFeB became even and the porosity decreased.

The cross-sectional morphologies and thicknesses of the bare NdFeB, EP/NdFeB and ZnAl-EP/NdFeB are shown in Fig. 2. It can be more intuitively observed from Fig. 2(a), the porosity of bare NdFeB is high, which means that the corrosive medium will more easily penetrate into the substrate and react with the chemically active Nd element. This will result in the failure of the magnet performance. As shown in Fig. 2(b), the EP coating is uniform and dense, and its thickness is

approximately  $10.5 \mu\text{m}$ . It can be clearly observed that the thickness of the ZnAl-EP coating is about  $30.5 \mu\text{m}$  (Fig. 2c). Due to its good fluidity and film-forming characteristics (Ref 25), when the epoxy resin was attached to the surface of ZnAl layer, some particles of the epoxy resin can enter the gaps of ZnAl layer. After the curing process, the EP layer and the ZnAl layer are closely combined to form a dense ZnAl-EP coating. It can be seen that there are no cracks or inclusions at the interface between the ZnAl-EP coating and the substrate, the fracture is not peeled off, and the bonding strength is high. In order to further examine the thickness of ZnAl-EP, a line scan was performed on the section of the ZnAl-EP/NdFeB magnetic. As can be seen from Fig. 2(d), the Fe element did not appear until  $30 \mu\text{m}$ , which is a convincing proof that the thickness of ZnAl-EP/NdFeB is about  $30 \mu\text{m}$ .

### 3.2 Potentiodynamic Polarization and EIS

Figure 3 shows the polarization curves of bare NdFeB, EP/NdFeB and ZnAl-EP/NdFeB. The black curve shows the potentiodynamic polarization of bare NdFeB, in which corrosion potential ( $E_{corr}$ ) reaches  $-1 \text{ V}$ . Compared with the bare NdFeB, the  $E_{corr}$  of EP/NdFeB and ZnAl-EP/NdFeB shift to the positive direction,  $-0.6$  and  $-0.78 \text{ V}$ , respectively. This indicates that both coatings are beneficial for retarding the

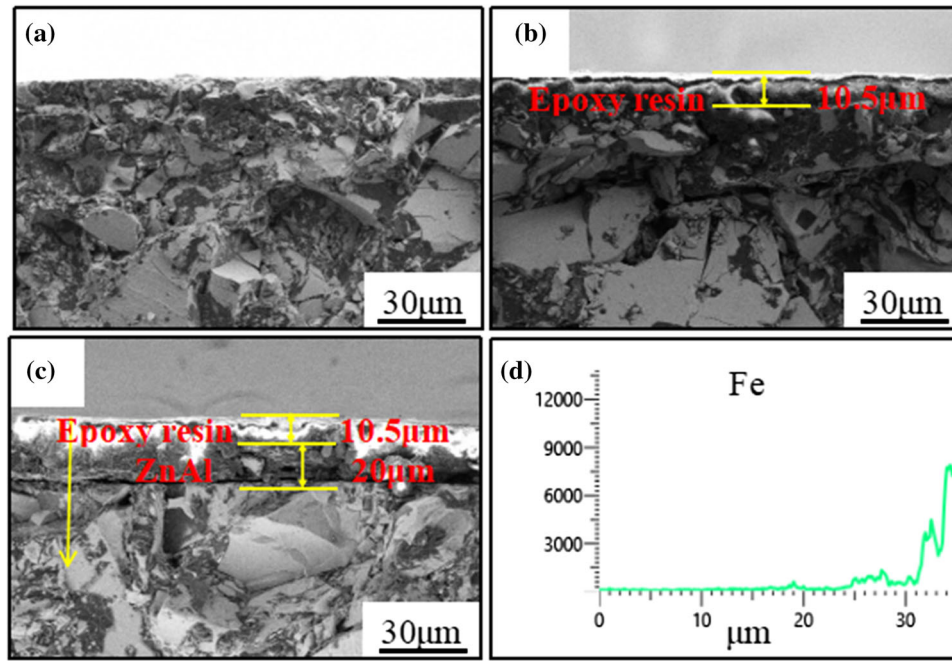


**Fig. 2** SEM section morphologies of bare NdFeB(a), EP/NdFeB (b) and ZnAl-EP/NdFeB( c); EDS line scanning analysis of ZnAl-EP/NdFeB (d)

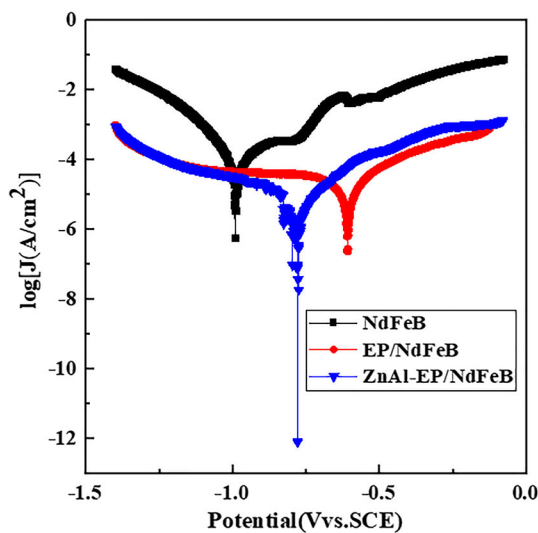


**Fig. 3** Potentiodynamic polarization curves of bare NdFeB, EP/NdFeB and ZnAl-EP /NdFeB

corrosion tendency of the magnets. Moreover, the  $E_{corr}$  of ZnAl-EP/NdFeB is more negative than that of EP/NdFeB, manifesting the easy corrosion tendency of ZnAl-EP/NdFeB in NaCl solution. This is on account of the ZnAl layer in ZnAl-EP/NdFeB having a passivation phenomenon on the anode side of the potentiodynamic polarization curve. The ZnAl layer reacts with the corrosive medium to form a passivation film, which can provide cathodic protection at the expense of the anode (Ref 26).

The polarization curves are analyzed by Tafel extrapolation, and  $E_{corr}$ ,  $J_{corr}$  and polarization resistance ( $R_{corr}$ ) obtained are listed in Table 1. The corresponding  $J_{corr}$  of bare NdFeB, EP/NdFeB and ZnAl-EP/NdFeB is  $1.033 \times 10^{-4}$ ,  $1.904 \times 10^{-5}$

and  $3.776 \times 10^{-6}$  A/cm<sup>2</sup>, respectively. The anode side is controlled by active dissolution reaction of bare NdFeB in NaCl solution, and  $J_{corr}$  builds up rapidly with the increase in the anode potential. The  $J_{corr}$  of ZnAl-EP/NdFeB is two orders of magnitude lower than that of bare NdFeB and one order of magnitude lower than that of EP/NdFeB. According to Faraday's law, the self-corrosion velocity is proportional to the corrosion current density (Ref 27). Compared to the bare NdFeB and the EP/NdFeB, the ZnAl-EP/NdFeB has the lowest  $J_{corr}$ , meaning that there are low self-corrosion velocity and good corrosion resistance properties. The lowest  $J_{corr}$  of the ZnAl-EP/NdFeB is owing to the outer layer of EP particles penetrating into the pores of the ZnAl layer, and the coating becomes dense and uniform. This structure prevents the corrosive medium from entering the substrate and further improves the corrosion resistance of the magnet.

The calculation formula of  $R_{corr}$  is shown in Formula 1 (Ref 28):

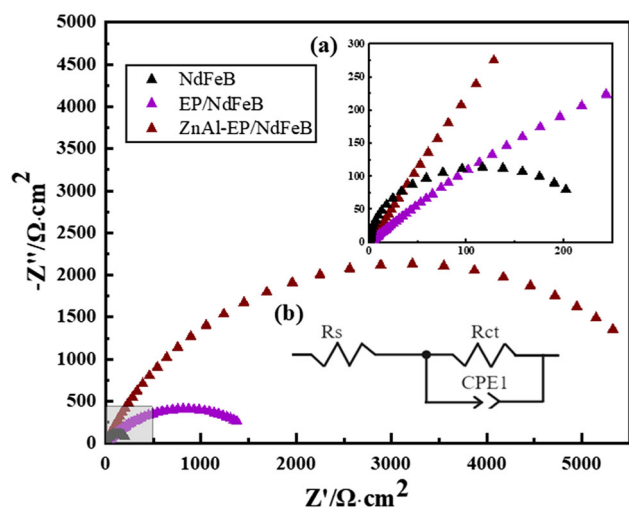
$$R_{corr} = \beta_a \cdot \beta_c / [2.303 \cdot I_{corr} \cdot (\beta_a + \beta_c)] \quad (\text{Eq 1})$$

where  $R_{corr}$  is the polarization resistance,  $\beta_a$  and  $\beta_c$  are the slopes of the polarization curves, and  $I_{corr}$  is the corrosion current. From the perspective of  $R_{corr}$ , the  $R_{corr}$  of ZnAl-EP/NdFeB reaches 23,219  $\Omega$ , which is much higher than the other two samples. This means that the ZnAl-EP/NdFeB has the optimum corrosion resistance.

The EIS was measured to further investigate the corrosion mechanism of bare NdFeB, EP/NdFeB and ZnAl-EP/NdFeB, as displayed in Fig. 4. In addition,  $R_s$  is the solution resistance and  $R_{ct}$  is the charge transfer resistance, respectively. To accurately fit the EIS results, constant phase angle element (CPE1) is used instead of the pure capacitance. Clearly, bare NdFeB, EP/NdFeB and ZnAl-EP/NdFeB all display only one high-frequency capacitor arc. It is worth noting that the diameter of high-frequency capacitor arc of ZnAl-EP/NdFeB

**Table 1 Polarization data of bare NdFeB, EP/NdFeB and ZnAl-EP /NdFeB**

Specimen	$E_{corr}$ , V	$J_{corr}$ , A/cm <sup>2</sup>	Cathodic slope	Anodic slope	$R_{corr}$ , $\Omega$
Bare NdFeB	- 1.00	$1.033 \times 10^{-4}$	9.436	4.789	704
EP/NdFeB	- 0.60	$1.904 \times 10^{-5}$	4.169	5.256	5570
ZnAl-EP/NdFeB	- 0.78	$3.776 \times 10^{-6}$	4.564	7.245	23,219

**Fig. 4** Electrochemical impedance spectrum of bare NdFeB, EP/NdFeB and ZnAl-EP /NdFeB, enlarged version of bare NdFeB (a), equivalent circuit model (b)**Table 2** Equivalent circuit fitting data of bare NdFeB, EP/NdFeB and ZnAl-EP /NdFeB

Specimen	$R_s$ , $\Omega \text{ cm}^2$	$R_{ct}$ , $\Omega \text{ cm}^2$
Bare NdFeB	0.4	237.0
EP/NdFeB	1.3	1671.6
ZnAl-EP/NdFeB	2.0	6316.0

is much larger than the other two samples. The increased radius of the resistance arc indicates an improvement in corrosion resistance. This demonstrates that ZnAl-EP/NdFeB has the best anti-corrosion performance than bare NdFeB and EP/NdFeB, which is consistent with the above conclusion.

Using the equivalent circuit (Ref 29) in Fig. 4(b) to fit the EIS results, the impedance data are listed in Table 2. The result of  $R_s$  demonstrates that the solution is relatively stable during the EIS test with the range from 0.4 to 2.0  $\Omega \cdot \text{cm}^2$ . Nonetheless, the change of  $R_{ct}$  is very significant. The  $R_{ct}$  of ZnAl-EP/NdFeB is 6316.0  $\Omega \cdot \text{cm}^2$ , while the  $R_{ct}$  of EP/NdFeB is only 1671.6  $\Omega \cdot \text{cm}^2$ . The  $R_{ct}$  value of ZnAl-EP/NdFeB is nearly four times that of EP/NdFeB, which can prove that the ZnAl-EP/NdFeB has the excellent anti-corrosion ability. In the comprehensive analysis of polarization curves and EIS, the results show that the ZnAl-EP/NdFeB has the best corrosion resistance, which is mainly due to the dense structure and the synergistic effect of the composite coating.

### 3.3 NSS Test

In order to further verify the corrosion resistance of the ZnAl-EP coating, the NSS test was carried out, and the results are shown in Fig. 5. When the bare NdFeB was exposed to the salt spray environment for 24 h, the surface of the magnet was found to be entirely covered with red products, indicating the NSS test time of bare NdFeB was less than 24 h (Fig. 5b). When the NSS time came up to 72 h, as shown in Fig. 5(e), a red rust spot appeared on the surface of EP/NdFeB, indicating that the EP/NdFeB is slightly corrupted at this time. The NSS time of EP/NdFeB was three times longer than that of bare NdFeB. At present, a single EP is rarely used to prepare protective coatings, and nanoparticle doping is generally required. Xu et al. (Ref 30) prepared a 40  $\mu\text{m}$  titanium nanoparticle-enhanced EP coating on sintered NdFeB surface by electrophoretic deposition, and its NSS time exceeded 600 h. Zhang et al. (Ref 31) prepared a  $\text{CeO}_2/\text{EP}$  composite coating on the surface of sintered NdFeB magnet and found that its NSS time can reach 1248 h. In order to be more flexible and convenient in the experiment, a single EP coating was prepared in this paper as a matched group, which may be insufficient in performance compared with other surveys. As can be seen from Fig. 5(h), the red spot appeared on the surface of ZnAl-EP/NdFeB after being exposed to a salt spray environment for 936 h. The NSS time of ZnAl-EP/NdFeB is one order of magnitude higher than that of bare NdFeB and EP/NdFeB, which means that the corrosion resistance of ZnAl-EP/NdFeB is greatly improved.

In addition, the surface morphologies of the samples after corrosion were analyzed in detail by SEM. As shown in Fig. 5(c), when the salt spray experiment lasted for 24 h, serious cracking and pulverization appeared on the surface of the bare NdFeB, and the crack size in local areas exceeded 10  $\mu\text{m}$ . Compared with the bare NdFeB, we can observe that although bubbling and falling off appeared on the surface of EP/NdFeB after corrosion (Fig. 5f), the overall surface of EP/NdFeB remained flat and still had good corrosion resistance. The reason for the bubbles and the shedding is owing to the reaction between the corrosive medium and the NdFeB substrate to generate corrosion products that make the coating bulge. When the salt spray experiment reached 936 h, the surface of the ZnAl-EP/NdFeB remained even and smooth (Fig. 5i), indicating that the composite coating still had good corrosion resistance. Therefore, ZnAl-EP composite coating is expected to become one of the alternatives of traditional coatings and become a kind of high corrosion resistance coating.

Since the surface of the bare NdFeB is loose and porous, this will inevitably speed up the process of the corrosive medium entering the substrate and reacting with the substrate. For the EP/NdFeB, the surface is flat and uniform, which has good corrosion resistance within a certain period. The ZnAl-EP/NdFeB has the best corrosion resistance, mainly ascribed to the

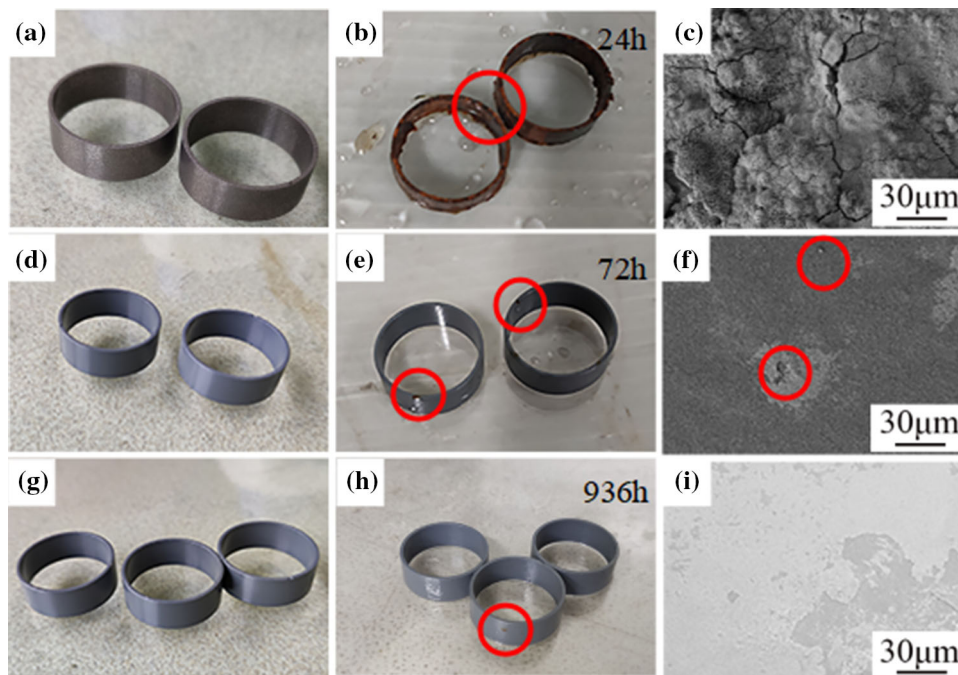


**Fig. 5** Physical pictures before and after corrosion and corrosion morphologies of bare NdFeB (a,b,c), EP/NdFeB (d,e,f) and ZnAl-EP/NdFeB (g,h,i)

synergistic effect of the composite coating. For one thing, the EP layer improves the structure of the ZnAl layer and makes its surface dense and uniform. For another, during the electrochemical reaction, ZnAl has the protective effect of the sacrificial anode, which further prevents the contact of corrosion products with the NdFeB substrate. We believe that this is a notable phenomenon and may also be an effective method to improve the corrosion resistance of bonded NdFeB magnets. The corrosion resistance mechanism of composite coating will be researched in detail in the future.

### 3.4 Magnetic Property

For magnets, the influence of surface coating on their magnetic properties is also an important issue to be considered in practice. Figure 6 and Table 3 are the magnetization curves and corresponding data of the bare NdFeB, EP/NdFeB and ZnAl-EP/NdFeB, respectively. As can be seen from Fig. 6, the  $B_r$  and  $H_{cj}$  values of both EP/NdFeB and ZnAl-EP/NdFeB are smaller than those of bare NdFeB. However,  $B_r$  and  $H_{cj}$  values of EP/NdFeB have little change compared with bare NdFeB values. Comparatively speaking, the  $H_{cj}$  value of ZnAl-EP/NdFeB decreases more than that of bare NdFeB. As shown in Table 3, the magnetic properties of the bare NdFeB are that the  $B_r$  is 6.62 kGs, the  $H_{cj}$  is 11.67 kOe, and the  $(BH)_{max}$  is 9.22 MGOe. But the  $H_{cj}$  and  $(BH)_{max}$  of ZnAl-EP/NdFeB were 10.60 kOe and 8.52 MGOe, respectively. Compared with bare NdFeB,  $H_{cj}$  and  $(BH)_{max}$  decreased by 9.1 and 7.6%, respectively.

Generally speaking, the protective coating on the NdFeB magnet surface is a non-magnetic phase, which has a particular effect on the magnetic properties of NdFeB magnet. For example, Chen et al. (Ref 32) reported that the NdFeB precipitation had a loss of coercivity by 24% due to the existence of the Ni-P coatings. But research on  $\text{SiO}_2/\text{NdFeB}$  showed that the  $\text{SiO}_2$  coating has a slight effect on the  $B_r$  of

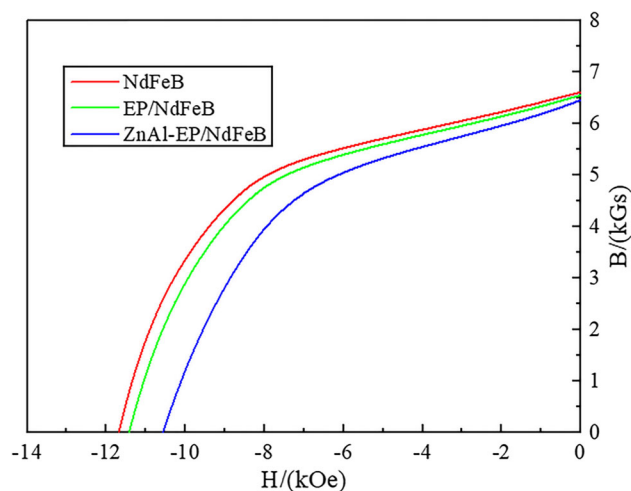


**Fig. 6** Magnetic properties of bare NdFeB, EP/NdFeB and ZnAl-EP/NdFeB

**Table 3** Magnetic properties of bare NdFeB, EP/NdFeB and ZnAl-EP/NdFeB

Specimen	$B_r$ , kGs	$H_{cj}$ , kOe	$(BH)_{max}$ , MGOe
Bare NdFeB	6.62	11.67	9.22
EP/NdFeB	6.60	11.60	9.16
ZnAl-EP/NdFeB	6.50	10.60	8.52

sintered NdFeB magnet (Ref 33). The EP coating prepared in this experiment has little impact on the magnetic properties of bonded NdFeB magnets. However, ZnAl-EP composite coating has a significant impact on the magnetic properties of bonded

NdFeB magnets, especially leading to a considerable decrease in the  $H_{cj}$  value. This is similar to the research results of Al-Mn coating (Ref 34). According to the current research results, due to the different composition and structure of coating, its influence on the magnetic properties of magnets is also distinct. Nevertheless, the specific influencing laws and mechanism analysis need to be further studied. This is also one of the essential topics in the future research of surface coating technology for bonded NdFeB magnets.

## 4. Conclusions

In this paper, ZnAl/EP composite coating was prepared on the surface of bonded NdFeB magnetic ring for the first time by air spraying combined with electrophoretic deposition process. Compared with the bare NdFeB and the EP/NdFeB, the ZnAl-EP/NdFeB was compact and homogeneous, which effectively prevented the corrosive medium from entering the NdFeB substrate and improved the anti-corrosion performance. The  $J_{corr}$  of the ZnAl-EP/NdFeB was one order of magnitude lower than that of the EP/NdFeB and 2 orders of magnitude lower than that of the bare NdFeB. The  $R_{corr}$  and the  $R_{ct}$  of ZnAl-EP/NdFeB were 23,219  $\Omega$  and 6316.0  $\Omega \cdot \text{cm}^2$ , respectively. The NSS resistance time of the ZnAl-EP/NdFeB coating reached 936 h. Furthermore, the ZnAl-EP coating has no significant effect on magnetic properties of NdFeB magnetic ring.

## Acknowledgments

The authors gratefully acknowledge the financial support of the project from Hefei Key Technology Research and Development Project (J2020G20) and the Key Research and Development Program of Anhui Province (202104A05020001).

## References

1. J. Huang, Q. Liu, Z.Y. Yang, G.Q. Xu, P.J. Zhang and J. Lv, Densification and Anticorrosion Performances of Vacuum Evaporated Aluminium Coatings on NdFeB Magnets, *J. Rare Earths.*, 2021, **39**, p 1238–1245. <https://doi.org/10.1016/j.jre.2020.11.014>
2. S.S. Lin, Y.F. Su, K.W. Song, F. Hu, Q. Shi and H.J. Hou, Influence of Transition Layer on Corrosion Resistance of Vaporized Aluminum Coating on NdFeB Surface, *Surf. Technol.*, 2017, **12**, p 228–234. <https://doi.org/10.16490/j.cnki.issn.1001-3660.2017.12.034>
3. D.C. Nababan, R. Mukhlis, Y. Durandet, M.I. Pownceby, L. Prentice and M.A. Rhamdhani, Mechanism and Microstructure Evolution of High Temperature Oxidation of End-of-life NdFeB Rare Earth Permanent Magnets, *Corro. Sci.*, 2021, **182**, 109290. <https://doi.org/10.1016/j.corsci.2021.109290>
4. J. Chen, H.Y. Yang, G.Q. Xu, P.J. Zhang, J. Lv and W. Sun, Rare Earth Passivation and Corrosion Resistance of Zinc Coated NdFeB Magnets, *J. Rare Earths.*, 2022, **40**(2), p 302–308. <https://doi.org/10.1016/j.jre.2020.11.012>
5. C.C. Ma, X.F. Liu and C.G. Zhou, Cold-sprayed Al Coating for Corrosion Protection of Sintered NdFeB, *J. Therm. Spray. Technol.*, 2014, **23**, p 456–462. <https://doi.org/10.1007/s11666-013-9994-8>
6. Z.Y. Cao, X.F. Ding, B. Robabeh, G.W. Abdul, C. Xu and L.J. Yang, The Deposition, Microstructure and Properties of Al Protective Coatings for NdFeB Magnets by Multi-arc Ion Plating, *Vacuum.*, 2017, **142**, p 37–44.
7. H. Parmar, T. Xiao, Z. Yaoying, V. Chaudhary, D.D. Peng and Y.Z. Huang, Improved Corrosion Resistance of Co, Al-alloyed NdFeB Magnetic Nanostructures Processed by Microwave Synthesis Techniques, *IEEE. Trans. Magn.*, 2018, **54**(11), p 1–5. <https://doi.org/10.1109/TMAG.2018.2838599>
8. E. Isotahdon, E. Huttunen-Saarivirta and V.T. Kuokkala, Characterization of the Microstructure and Corrosion Performance of Ce-alloyed Nd-Fe-B Magnets, *J. Alloys Compd.*, 2017, **692**, p 190–197. <https://doi.org/10.1016/j.jallcom.2016.09.058>
9. L.Q. Yu, Y.H. Wen and M. Yan, Effects of Dy and Nb on the Magnetic Properties and Corrosion Resistance of Sintered NdFeB, *J. Magn. Mater.*, 2004, **283**, p 353–356. <https://doi.org/10.1016/j.jmmm.2004.06.006>
10. W. Liu and J. Hou, Production Status and Prospect of NdFeB Magnet Electroplating, *Plat. Finish.*, 2012, **34**(4), p 20–26. <https://doi.org/10.1055/s-0032-1311839>
11. Y.Q. Huang, H.Q. Li, M. Zuo, L. Tao, W. Wang, J. Zhang and Q. Tang, Corrosion Resistance of Sintered NdFeB Coated with SiC/Al Bilayer Thin Films by Magnetron Sputtering, *J. Magn. Mater.*, 2016, **409**, p 39–44. <https://doi.org/10.1016/j.jmmm.2016.02.006>
12. Q.J. Liu, P.J. Zhang, M.H. Wang, W.F. Wang, J.Q. Liu and Y.C. Wu, Properties of Carbon Nano-tube/epoxy resin Composite Coating on Sintered NdFeB Magnets, *Heat. Treat. Metal.*, 2016, **1**, p 179–183. <https://doi.org/10.13251/j.issn.0254-6051.2016.01.038>
13. S.D. Mao, H.X. Yang, F. Huang, T.T. Xie and Z.L. Song, Corrosion Behaviour of Sintered NdFeB Coated with Al/Al<sub>2</sub>O<sub>3</sub> Multilayers by Magnetron Sputtering, *Appl. Surf. Sci.*, 2011, **257**, p 3980–3984. <https://doi.org/10.1016/j.apsusc.2010.11.162>
14. S.J. Wang, T.T. Xie, C. Yu and Z.L. Song, Microstructure and Corrosion Resistance of Ionic Liquid Electrodeposited Al Layer on NdFeB Magnet, *Mater. Protect.*, 2012, **70**, p 1–3. <https://doi.org/10.16577/j.cnki.42-1215/tb.2012.08.005>
15. P.J. Zhang, J.Q. Liu, G.Q. Xu, X.F. Yi, J.W. Chen and Y.C. Wu, Anticorrosive Property of Al Coatings on Sintered NdFeB Substrates Via Plasma Assisted Physical Vapor Deposition Method, *Surf. Coat. Technol.*, 2015, **282**, p 86–93. <https://doi.org/10.1016/j.surfcoat.2015.10.021>
16. J.W. Zheng, M. Lin and Q.P. Xia, A preparation Method and Effects of Al-Cr Coating on NdFeB Sintered Magnets, *J. Magn. Mater.*, 2012, **324**, p 3966–3969. <https://doi.org/10.1016/j.jmmm.2012.07.006>
17. F.Q. Lang and Z.M. Yu, The Corrosion Resistance and Wear Resistance of Thick TiN Coatings Deposited by Arc Ion Plating, *Surf. Coat. Technol.*, 2001, **145**, p 80–87. [https://doi.org/10.1016/S0257-8972\(01\)01284-1](https://doi.org/10.1016/S0257-8972(01)01284-1)
18. J.L. Li, S.D. Mao, K.F. Sun, X.M. Li and Z.L. Song, AlN/Al Dual Protective Coatings on NdFeB by DC Magnetron Sputtering, *J. Magn. Mater.*, 2009, **321**, p 3799–3803. <https://doi.org/10.1016/j.jmmm.2009.07.039>
19. P.J. Zhang, P.J. Cao, W. Sun, B.S. Li, Y.C. Wu and G.Q. Xu, Synthesis and Corrosion Resistance of CeO<sub>2</sub>/silane Composite Coatings on Surface of Sintered NdFeB Magnet, *Transact. Mater. Heat. Treat.*, 2020, **41**, p 123–131. <https://doi.org/10.13289/j.issn.1009-6264.2019-0350>
20. F. Liu, Q. Li, X.K. Yang, Y. Dai, F. Luo, S.Y. Wang and H.X. Zhang, Corrosion Resistance of Environment-friendly Sealing Layer for Zn-coated Sintered NdFeB Magnet, *Mater. Corros.*, 2011 <https://doi.org/10.1002/maco.201006039>
21. J. Chen, J.L. Xu, J. Huang, J. Dai, M.S. Xue and J.M. Luo, Corrosion Resistance of T-ZnOw/PDMS-MAO Composite Coating on the Sintered NdFeB Magnet, *J. Magn. Mater.*, 2021, **534**, 168049. <https://doi.org/10.1016/j.jmmm.2021.168049>
22. T.C. Chen, C.C. Chou, T.Y. Yung, K.C. Tsai and J.Y. Huang, Wear Behavior of Thermally Sprayed Zn/15Al, Al and Inconel 625 Coatings on Carbon Steel, *Surf. Coat. Technol.*, 2016, **303**, p 78–85. <https://doi.org/10.1016/j.surfcoat.2016.03.095>
23. Y.J. Cao, Y.H. Liu, P.J. Zhang, G.Q. Xu, J.Q. Liu, X.F. Yi and Y.C. Wu, Effects of CeO<sub>2</sub> Nanoparticles Doping on Properties of Zn-Al Coating on Sintered NdFeB Magnets, *China. Surf. Eng.*, 2020, **33**, p 100–107.
24. Y.W. Yang, Y.L. Wang, L. Yang, R.D. Ren, J.G. Liu and X.G. Fang, The Preparation and Properties of ZnAl Coating for Ring-shaped Bonded NdFeB Magnet with High Corrosion Resistance, *J. Mater. Eng. Perform.*, 2022, **31**, p 1003–1008. <https://doi.org/10.1007/s11665-021-06259-1>
25. S.A. He, S.A. Zhu, Z. Zheng and Y.X. Li, The Film-forming Property and Modification Effect on Ultra-high Performance Concrete of Epoxy Resin Emulsion, *J. Hans. Civil. Eng.*, 2016, **5**, p 253–261. <https://doi.org/10.12677/HJCE.2016.56034>

26. J.J. Ding, B.J. Xu and G.P. Ling, Al-Mn Coating Electrodeposited from Ionic Liquid on NdFeB Magnet with High Hardness and Corrosion Resistance, *Appl. Surf. Sci.*, 2014, **305**, p 309–313. <https://doi.org/10.1016/j.apsusc.2014.03.067>
27. J. Chen, H.Y. Yang, G.Q. Xu, P.J. Zhang, J. Lv, W. Sun and B.S. Li, Phosphating Passivation of Vacuum Evaporated Al/NdFeB Magnets Boosting High Anti-corrosion Performances, *Surf. Coat. Technol.*, 2020, **399**, 126115. <https://doi.org/10.1016/j.surfcoat.2020.126115>
28. J.M. Xiao and C.N. Cao, Principles of Material Corrosion, *Chem. Indust. Publish.*, 2002, **1**, p 32–33. (in Chinese)
29. L.Z. Song and Z.Y. Yang, Corrosion Resistance of Sintered NdFeB Permanent Magnet with Ni-P/TiO<sub>2</sub> Composite Film, *J. Iron. Steel. Res.*, 2009, **16**, p 89–94. <https://doi.org/10.13228/j.boyuan.issn1006-706x.2009.03.007>
30. J.L. Xu, Z.X. Huang, J.M. Luo and Z.C. Zhong, Effect of Titania Particles on the Microstructure and Properties of the Epoxy Resin Coatings on Sintered NdFeB Permanent Magnets, *J. Magn. Magn. Mater.*, 2014, **355**, p 31–36. <https://doi.org/10.1016/j.jmmm.2013.11.050>
31. P.J. Zhang, M.G. Zhu, W. Li, G.Q. Xu, X.L. Huang, X.F. Yi, J.W. Chen and Y.C. Wu, Study on Preparation and Properties of CeO<sub>2</sub>/Epoxy resin Composite Coating on Sintered NdFeB Magnet, *J. Rare Earths.*, 2018, **36**, p 544–551. <https://doi.org/10.1016/j.jre.2017.11.012>
32. Z. Chen, A. Ng, J.Z. Yi and X.F. Chen, Multi-layered Electroless Ni-P Coatings on Powder-sintered Nd-Fe-B Permanent Magnet, *J. Magn. Magn. Mater.*, 2006, **302**, p 216–222. <https://doi.org/10.1016/j.jmmm.2005.09.008>
33. J.L. Xu, Q.F. Xiao, D.D. Mei, Z.C. Zhong, Y.X. Tong, Y.F. Zheng and L. Li, Preparation and Characterization of Amorphous SiO<sub>2</sub> Coatings Deposited by Micro-arc Oxidation on Sintered NdFeB Permanent Magnets, *J. Magn. Magn. Mater.*, 2017, **426**, p 361–368. <https://doi.org/10.1016/j.jmmm.2016.11.105>
34. J.J. Ding, B.J. Xu and G.P. Ling, Al-Mn Coating Electrodeposited from Ionic Liquid on NdFeB Magnet with High Hardness and Corrosion Resistance, *Appl. Surf. Sci.*, 2014, **305**, p 309–313. <https://doi.org/10.1016/j.apsusc.2014.03.067>

**Publisher's Note** Springer Nature remains neutral with regard to jurisdictional claims in published maps and institutional affiliations.